Available online at www.sciencedirect.com
ScienceDirect
Dyes and Pigments 77 (2008) 59–69
DYES and PIGMENTS
www.elsevier.com/locate/dyepig

Flexible zinc oxide solar cells sensitized by styryl dyes

Takuya Dentani [a], Ken-ichi Nagasaka [a], Kazumasa Funabiki [a], Ji-Ye Jin [b], Tsukasa Yoshida [c], Hideki Minoura [c], Masaki Matsui [a,*]

[a] Department of Materials Science and Technology, Faculty of Engineering, Gifu University, Yanagido, Gifu 501-1193, Japan
[b] Department of Chemistry, Faculty of Science, Shinshu University, 3-1-1 Asahi, Matsumoto, Nagano 390-8621, Japan
[c] Environmental and Renewable Energy System Division, Graduate School of Engineering, Gifu University, Yanagido, Gifu 501-1193, Japan

Received 23 October 2006; received in revised form 1 March 2007; accepted 13 March 2007
Available online 6 April 2007

Abstract

Application of a series of styryl dyes for flexible zinc oxide solar cells prepared by the one-step cathode deposition template method was examined. 3-(2-Carboxyethyl)-2-[4-(dimethylamino)styryl]benzothiazolium iodide (**27**) showed the best performance as the sensitizer. The incident photon-to-current efficiency (IPCE) at around 490 nm, maximum short-circuit photocurrent density (J_{sc}), open-circuit photovoltage (V_{oc}), fill factor (ff), and solar-light-to-electricity conversion efficiency (η) were observed to be 54.5%, 6.22 mA cm^{-2}, 0.53 V, 0.59, and 1.94%, respectively.

Keywords: Flexible film; Zinc oxide solar cell; Sensitizer; Styryl dye

1. Introduction

Much attention has been paid to the survey of sensitizers for dye-sensitized solar cells [1]. Coumarin [2], merocyanine [3], polyene [4], and indoline dyes [5] were reported to act as good sensitizers for titanium oxide. Styryl dyes having a propylsulfonate and carboxymethyl group as the anchor moiety were also reported as the sensitizers for titanium oxide solar cells [6,7]. Since high temperature process is not used for conductive plastic substrates, mechanical compression of crystalline particle [8], electron beam shower exposure [9], microwave irradiation [10], hydrothermal crystallization [11], high-field electrophoretic deposition [12], and spray deposition and compression methods [13] were proposed for flexible titanium oxide solar cells. In most cases, ruthenium complexes are used as the sensitizers for titanium oxide. Meanwhile, the application of zinc oxide in dye-sensitized solar cells was also reported [14]. Recently, convenient method for the preparation of zinc oxide film was described, called the ''one-step cathode deposition'' [15]. The good point of this method is the formation of porous zinc oxide film at low temperature (<70 °C). Therefore, zinc oxide prepared by this method can be used as the semiconductor in flexible dye-sensitized solar cells. In this paper, styryl dyes were screened as the sensitizers. Then, by using the best dye selected, the preparation method of flexible zinc oxide solar cell was examined to improve cell performance.

2. Results and discussion

2.1. Synthesis of dyes

Styryl dyes **23**–**33** were synthesized as shown in Scheme 1. Nitrogen-containing heteroaromatic compounds **1**–**4** reacted with chloro-, bromo-, and iodo-substituted carboxylic acids **5**–**8** to give *N*-(carboxyalkyl)heteroaromatic halides **11**–**15**, **18**, and **19**. Compound **1** also reacted with bromo-substituted ethyl esters **9** and **10** to afford *N*-alkoxycarbonylalkyl derivatives **16′** and **17′**, whose ester linkage was hydrolyzed to

* Corresponding author. Fax: +81 58 293 2601.
E-mail address: matsui@apchem.gifu-u.ac.jp (M. Matsui).

0143-7208/$ - see front matter © 2007 Elsevier Ltd. All rights reserved.
doi:10.1016/j.dyepig.2007.03.007

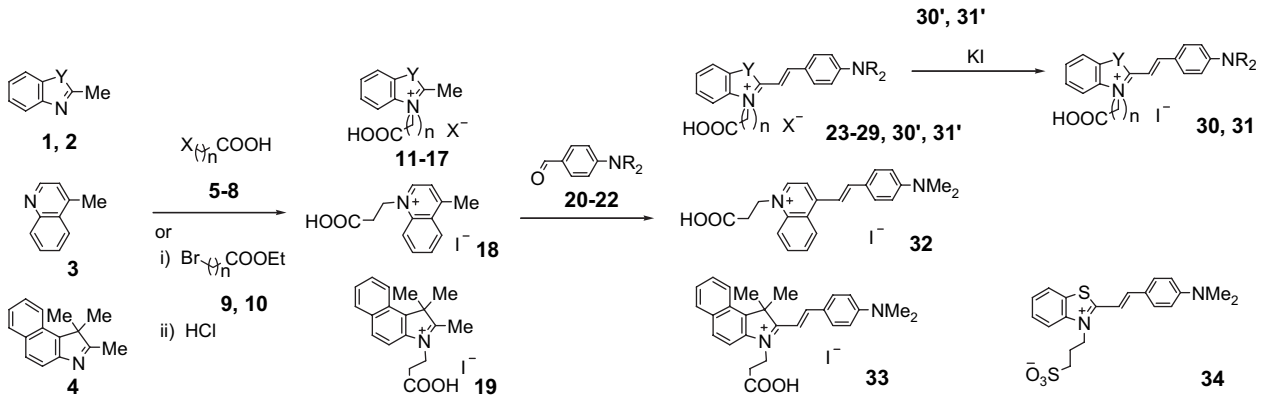

Compd	Y
1	S
2	CMe_2

Compd	n	X
5	1	Cl
6	1	Br
7	1	I
8	2	I
9	3	Br
10	4	Br

Compd	Y	n	X
11	S	1	Cl
12	S	1	Br
13	S	1	I
14	CMe_2	2	I
15	S	2	I
16	S	3	Br
17	S	4	Br

Compd	R
20	Me
21	Hex
22	Dodec

Compd	Y	n	X	R
23	S	1	Cl	Me
24	S	1	Br	Me
25	S	1	I	Me
26	CMe_2	2	I	Me
27	S	2	I	Me
28	S	2	I	Hex
29	S	2	I	Dodec
30'	S	3	Br	Me
30	S	3	I	Me
31'	S	4	Br	Me
31	S	4	I	Me

Scheme 1.

give the corresponding *N*-carboxyalkyl derivatives **16** and **17**, respectively. Then, compounds **11**–**19** reacted with aromatic aldehydes **20**–**22** to afford **23**–**29**, **30′**, **31′**, **32**, and **33** in low to moderate yields. Bromides **30′** and **31′** were treated with potassium iodide to give the iodides **30** and **31**, respectively. 2-[4-(Dimethylamino)styryl]benzothiazolium propylsulfonate (**34**) was prepared as described in the literature [6].

2.2. Preparation of preliminary flexible zinc oxide solar cell for screening of styryl dyes 23–33

Eosin Y-desorbed zinc oxide film (thickness: *ca*. 3 μm) was prepared as described in the literature [14]. The electro-deposition was carried out at 70 °C. The film was dried at 100 °C for 1 h. The desorbed zinc oxide film was immersed in an acetonitrile–*tert*-butyl alcohol 1:1 mixed solution (10 ml) of **27** (1×10^{-4} mol dm^{-3}) at 25 °C for 24 h. Then, the re-adsorbed zinc oxide film on conductive PET film was washed with an acetonitrile–*tert*-butyl alcohol 1:1 mixed solution and dried at ambient temperature under an air atmosphere. The film was used as the working electrode. Platinum spattered PET film was used as a counter electrode. UV-curing resin was put by hand around the cell. An acetonitrile–ethylene carbonate (v/v = 1:4) mixed solution containing tetrabutylammonium iodide (0.5 mol dm^{-3}) and iodine (0.05 mol dm^{-3}) was used as an electrolyte. AM 1.5 simulated sunlight (100 mW cm^{-2}) was irradiated through a shading mask (5.0 mm × 4.0 mm) to measure the cell performance.

2.3. Screening of styryl dyes

Styryl dyes **23**–**34** consist of electron-withdrawing heteroaromatic, electron-donating 4-(dialkylamino)phenyl, anchor and counter anion moieties, all of which can affect cell performance.

Firstly, the effect of heteroaromatic moiety on cell performance was examined. The UV–vis absorption and action spectra of **26**, **27**, **32**, and **33** are shown in Fig. 1. The results of the spectral data and cell performance of **23**–**34** are shown in Table 1. The incident photon-to-current efficiency (IPCE) and solar-light-to-electricity conversion efficiency (η) values of benzothiazolium derivative **27** (38.6 and 1.18%) were larger than those of 3*H*-indolium **26** (19.6 and 0.56), quinolinium **32** (19.9 and 0.73) and benzoindolium **33** (18.8 and 0.42) derivatives (runs 4, 5, 16, and 17). Their UV–vis absorption spectra on zinc oxide were broad compared with those in DMSO, suggesting the formation of aggregates on zinc oxide as shown in Fig. 1a. Interestingly, the UV–vis absorption spectra of **27** and **32** on zinc oxide showed hypsochromic shift whereas those of **26** and **33** did not. The E_{red} of **26** (−1.16 V) and **33** (−1.16) was slightly positive compared with that of **27** (−1.24) (runs 4, 5, and 17). The fluorescence intensity of **32** was very small (RFI = 9) compared with that of **27** (100) (runs 5 and 16). The E_{ox} of **32** was slightly negative (0.44) compared with that of **27** (0.52). These properties might attribute to less efficiency of electron injection from the excited dye to zinc oxide, resulting in the best performance of **27** among **26**, **27**, **32**, and **33**.

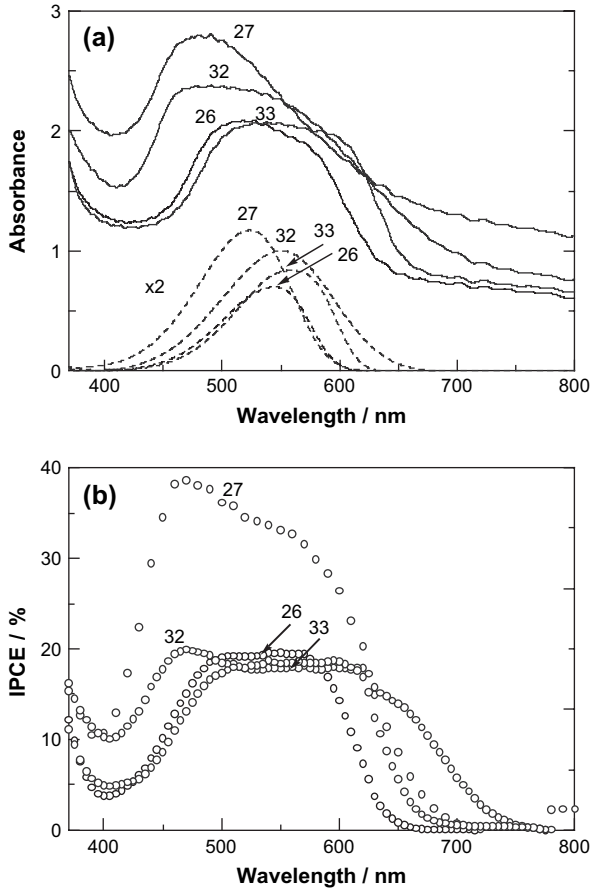

Fig. 1. (a) UV–vis absorption and (b) action spectra of **26**, **27**, **32**, and **33**. Solid and dotted lines represent the UV–vis absorption spectra on zinc oxide and in DMSO (1.0×10^{-5} mol dm^{-3}), respectively. The absorbance in DMSO is two-times large as measured.

Secondly, the effect of dialkylamino group on cell performance was examined. The UV–vis absorption and action spectra of **27**, **28**, and **29** are shown in Fig. 2. The IPCE and η values were in the following order: **27** (38.6 and 1.18%) > **28** (23.5 and 0.67) > **29** (17.3 and 0.42) (runs 5, 10, and 12). Thus, the IPCE and η values were higher as shorter was the alkyl groups at the dialkylamino moiety. The absorbance of dyes on zinc oxide film also increased in the order: **27** (2.81) > **28** (2.03) > **29** (1.34), suggesting that the cell performance was better with increasing amount of dye on zinc oxide (runs 5, 10, and 12). However, even when the amount of dye was similar, the cell performance of **27** was best followed by **28** and **29** (runs 6, 11, and 13). In Fig. 2a, the hypsochromic shift of **27** was observed whereas that of **28** and **29** was not. It is clear that the sensitization occurs at the hypsochromic band as shown in Figs. 1b and 2b. The hypsochromic shift on zinc oxide can come from either the decrease in electron-withdrawing nature of 2-carboxyethyl moiety due to the formation of carboxylate as reported in the case of coumarin derivatives on titanium oxide [16] or the aggregation formation on zinc oxide as reported for phenyl-conjugated oligoene derivatives [17]. No change in the UV–vis absorption spectrum of **27** in DMSO and ethanol was observed in the presence of 0–100 molar amounts of TEA and sodium hydroxide. This result suggested that the formation of carboxylate in styryl dyes **23**–**33** on zinc oxide did not cause hypsochromic shift. With increasing amount of deoxycholic acid (DCA), which is used as the coadsorbate, the amount of **27** on zinc oxide decreased, and at the same time, the IPCE and η values also decreased (runs 5, 7, 8, and 9). No change in the UV–vis absorption band of **27** on zinc oxide was observed by addition of DCA except for decrease in the absorbance. To our knowledge, no paper of aggregation formation of styryl dyes has been reported. It was reported that a monomer cyanine dye could dimerize in the range of the concentration 1.6–80×10^{-6} mol dm^{-3} in water and that the cyanine dye forms J-aggregates by the addition of potassium chloride [18]. The UV–vis absorption spectra of **27** in a DMSO–water mixed solution containing sodium chloride are shown in Fig. 3. By adding sodium chloride, the absorption band caused hypsochromic shift with decreasing absorbance. This result indicated that the styryl dye **27** could form the dimer and/or H-aggregates in solution. However, dimers and H-aggregates can deactivate the excited state to decrease cell performance. Therefore, in this stage, it is not clear why high IPCE value is observed at short wavelength on zinc oxide.

Thirdly, the effect of anchor group on cell performance was examined. The UV–vis absorption and action spectra of **25**, **27**, **30**, **31**, and **34** are shown in Fig. 4. All the UV–vis absorption spectra showed hypsochromic shift on zinc oxide as shown in Fig. 4a. 2-Carboxyethyl derivative **27** showed better performance (IPCE: 38.6 and η: 1.18%) than propylsulfonate derivative **34** (0.9 and 0.54) (runs 5 and 18). This result came from less affinity of **34** for zinc oxide. Better performance was obtained for the carboxymethyl **25** (IPCE: 34.6, η: 1.00) and 2-carboxyethyl derivatives **27** (38.6 and 1.18) than the 3-carboxypropyl **30** (21.7 and 0.72) and 4-carboxybutyl derivatives **31** (19.2 and 0.57) (runs 3, 5, 14, and 15). It was reported that the electron injection of carboxymethyl derivative into titanium oxide was more efficient than that of the 3-sulfonatopropyl derivative due to short distance between the dye chromophore and titanium oxide [7]. It is of interest that not only carboxymethyl but also 2-carboxyethyl derivatives show good performance for zinc oxide.

Finally, the effect of counter anion on cell performance was examined. The UV–vis absorption and action spectra of **23**, **24**, and **25** are shown in Fig. 5. The iodide **25** (IPCE: 34.6 and η: 1.00%) showed better performance than the chloride **23** (9.9 and 0.41) and bromide **24** (8.6 and 0.37) (runs 1–3). The E_{red} of **23** (−0.90 V) and **24** (−0.94) were positive compared with that of **25** (−1.33), which could result in less electron injection into zinc oxide (runs 1–3).

Thus, compound **27** was found to show the best performance among **23**–**34** for flexible zinc oxide solar cell prepared by the one-step cathode deposition template method.

2.4. Improved preparation method of flexible zinc oxide solar cell

An aqueous potassium chloride solution (300 ml, 0.1 mol dm^{-3}) was electrolyzed at −1.0 V *vs* SCE with bubbling an

Table 1
Physical properties and screening of styryl dyes

Run	Compound	λ_{max} (ε)[a], nm	λ_{em} (RFI)[a], nm	E_{ox}[b], V	E_{red}[b], V	λ_{max}c, nm	Absorbance[c]	IPCE[d], %	J_{SC}[d], mA cm^{-2}	V_{OC}[d], V	ff[d]	η[d], %
1	**23**	515 (54600)	606 (187)	0.87	−0.90	476	1.39	9.9	1.83	0.48	0.47	0.41
2	**24**	515 (59100)	605 (205)	0.84	−0.94	487	1.91	8.6	1.62	0.47	0.48	0.37
3	**25**	515 (54400)	609 (177)	0.44	−1.33	492	2.36	34.6	4.73	0.48	0.44	1.00
4	**26**	544 (35000)	604 (68)	0.56	−1.16	527	2.09	19.6	2.61	0.49	0.44	0.56
5	**27**	524 (57300)	610 (100)	0.52	−1.24	490	2.81	38.6	5.68	0.49	0.42	1.18
6	**27**	–	–	–	–	476	1.02	42.8	5.70	0.45	0.43	1.12
7	**27**[e]	–	–	–	–	481	2.13	29.0	3.24	0.52	0.47	0.79
8	**27**[f]	–	–	–	–	480	1.97	20.2	2.23	0.51	0.51	0.58
9	**27**[g]	–	–	–	–	482	1.46	13.6	2.02	0.51	0.48	0.50
10	**28**	541 (74300)	602 (271)	0.49	−1.29	523	2.03	23.5	3.32	0.49	0.41	0.67
11	**28**	–	–	–	–	536	1.00	24.0	3.11	0.50	0.41	0.65
12	**29**	541 (64600)	601 (340)	0.52	−1.26	510	1.34	17.3	1.95	0.52	0.41	0.42
13	**29**	–	–	–	–	547	0.91	22.7	2.43	0.51	0.39	0.49
14	**30**	526 (55600)	612 (165)	0.49	−1.29	478	2.95	21.7	3.75	0.47	0.41	0.72
15	**31**	528 (61100)	609 (97)	0.48	−1.29	482	2.28	19.2	2.89	0.47	0.42	0.57
16	**32**	550 (50000)	697 (9)	0.44	−1.26	491	2.38	19.9	4.25	0.47	0.36	0.73
17	**33**	559 (41900)	619 (144)	0.58	−1.16	539	2.08	18.8	2.81	0.46	0.33	0.42
18	**34**	529 (53000)	613 (146)	–[h]	–[h]	460	1.75	0.9	0.28	0.14	0.44	0.54

[a] Measured in DMSO at the concentration of 1×10^{-5} mol dm^{-3}.
[b] *vs* SCE in acetonitrile.
[c] On zinc oxide film.
[d] Action spectrum under monochromatic light with 0.05×10^{16} photon cm^{-2} s^{-1} and I–V characteristics under white light with 100 mW cm^{-2}.
[e] Dye **27** was immersed in the presence of DCA (1×10^{-3} mmol dm^{-3}).
[f] Dye **27** was immersed in the presence of DCA (3×10^{-3} mmol dm^{-3}).
[g] Dye **27** was immersed in the presence of DCA (5×10^{-3} mmol dm^{-3}).
[h] Not measured.

oxygen gas at 50 °C for 40 min. Platinum spattered PET film was used as a counter electrode. To the pre-electrolyzed film was added an aqueous solution of zinc chloride. The concentration of zinc oxide was adjusted to 5 mmol dm^{-3}. Then, the film was electro-deposited again in the solution at −1.0 V *vs* SCE at 50 °C for 10 min with bubbling an oxygen gas (pre-electrolysis process). Zinc was used as a counter electrode. To the electro-deposited film was added an aqueous solution of eosin Y. The concentration of eosin Y was adjusted to 40 μmol dm^{-3}. The film was electro-deposited at −1.0 V *vs* SCE at 50 °C for 30 min with bubbling an oxygen gas (electro-deposition process). Zinc was used as a counter electrode. The film was kept in a diluted aqueous potassium hydroxide (pH 10.5) for 24 h to remove adsorbed eosin Y. The film was dried at 100 °C for 1 h with pressing (drying process). The thin film was immersed into the chloroform solution of dye (1×10^{-4} mol dm^{-3}) and kept at 25 °C for 24 h to adsorb dye **27**. Then, the film was kept in the electrolyte solution for 1 h, washed with ethanol, and dried under an air atmosphere at ambient temperature (washing of **27**-adsorbed film process). UV-curing resin as spacer was supplied by using a robot (resin process). An acetonitrile–ethylene carbonate mixed solution (v/v = 1:4) of tetrapropylammonium iodide (0.5 mol dm^{-3}) and iodine (0.05 mol dm^{-3}) was used as an electrolyte. An action spectrum was measured under monochromatic light with a constant photon number (0.05×10^{16} photon cm^{-2} s^{-1}). I–V characteristics were measured under illumination with AM 1.5 simulated sunlight (100 mW cm^{-2}) through a shading mask (5.0 mm × 4.0 mm). The cell structure is shown in Fig. 6.

2.5. Flexible zinc oxide solar cell performance after improved preparation

The results of cell performance after improvement of cell preparation using **27** are shown in Table 2. In the case of flexible substrates, rolling of conductive PET film was observed during drying process. To improve this point, eosin Y-desorbed film was dried under pressing. Furthermore, to supply the constant amount of UV-curing resin, which acts as a spacer between the platinum spattered conductive PET and PET substrate, a robot was used (resin process). As a result, the fill factor was drastically improved to increase the η value (runs 1 and 2). When the immerse solvent, in which dye **27** is adsorbed on eosin Y-desorbed zinc oxide, was substituted from acetonitrile–*tert*-butyl alcohol (1:1) mixed solvent to chloroform, J_{sc} and V_{oc} values increased to improve η value (runs 2 and 3). To increase the amount of hydroxy ion, which is essential to prepare zinc oxide, electrolysis were carried out for 40 min with bubbling an oxygen gas. Then, second electrolysis was carried out for 10 min (pre-electrolysis process). Though the fill factor was slightly improved, J_{sc} and V_{oc} values decreased, resulting in no drastic improvement of η value (runs 3 and 4). When 4-*tert*-butylpyridine (TBP) was added to the electrolyte, J_{sc} value decreased (runs 4 and 5). When dye **27**-adsorbed zinc oxide film was kept in the electrolyte solution and then washed with ethanol to remove non-adsorbed excess **27**, the J_{sc} value increased to improve the η value (runs 4 and 6). When the pre-electrolysis and electro-deposition processes were carried out at 50 °C, the zinc oxide film became transparent resulting

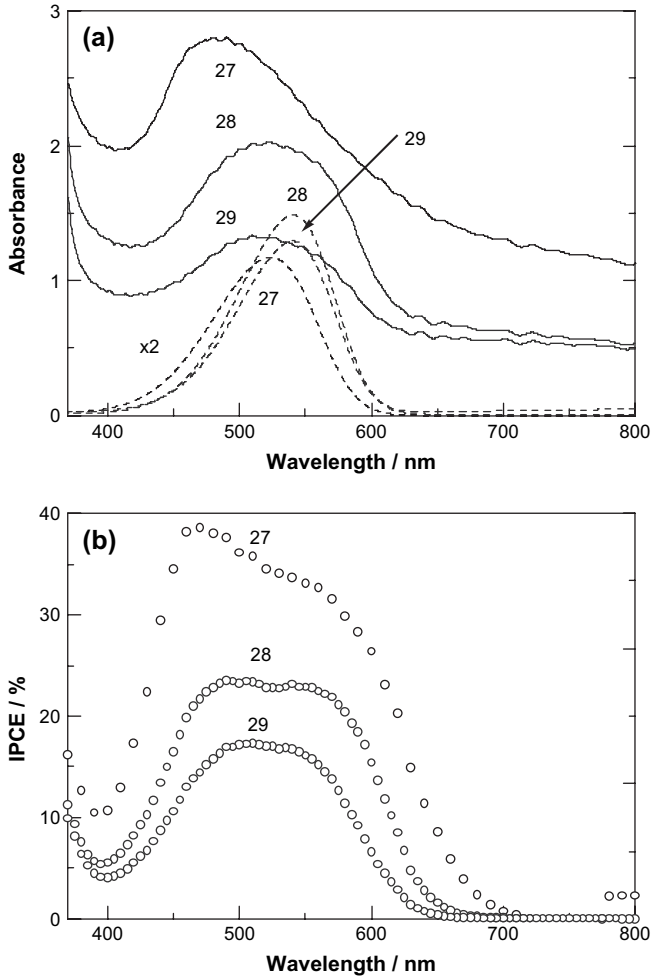

Fig. 2. (a) UV–vis absorption and (b) action spectra of **27**, **28**, and **29**. Solid and dotted lines represent the UV–vis absorption spectra on zinc oxide and in DMSO (1.0×10^{-5} mol dm^{-3}), respectively. The absorbance in DMSO is two-times large as measured.

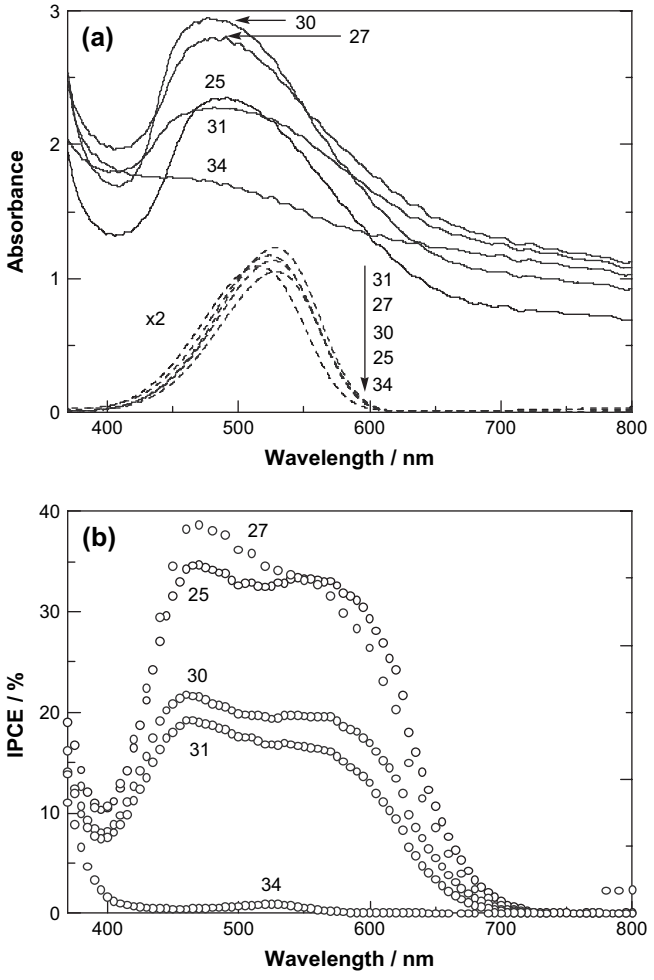

Fig. 4. (a) UV–vis absorption and (b) action spectra of **25**, **27**, **30**, **31**, and **34**. Solid and dotted lines represent the UV–vis absorption spectra on zinc oxide and in DMSO (1.0×10^{-5} mol dm^{-3}), respectively. The absorbance in DMSO is two-times large as measured.

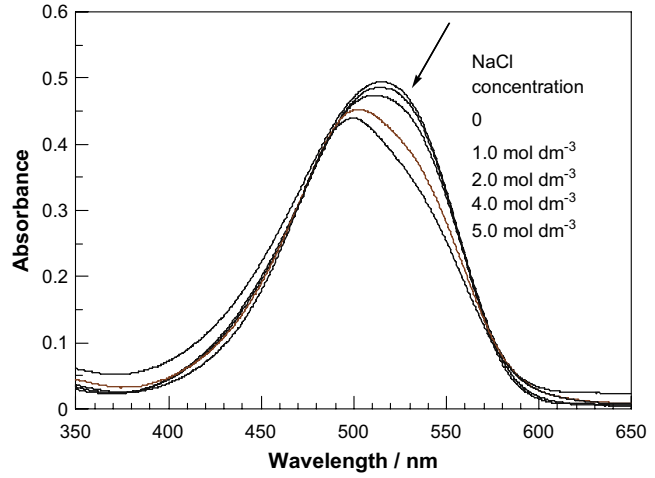

Fig. 3. UV–vis absorption band of **27** (1×10^{-5} mol dm^{-3}) in water in the presence of sodium chloride (0, 1.0, 2.0, 4.0, and 5.0 mol dm^{-3}).

in further improvement of fill factor to give the best cell performance (runs 6 and 7).

The UV–vis absorption and action spectra and photocurrent density–photovoltage (I–V) curve of **27** before (run 1 in Table 2) and after improvement (run 7 in Table 2) are shown in Figs. 7 and 8, respectively. The zinc oxide film became more transparent, and at the same time, the IPCE, J_{sc}, and V_{oc} values increased after improvement of cell preparation. The IPCE, J_{sc}, V_{oc}, ff, and η were calculated to be 54.5%, 6.22 mA cm^{-2}, 0.53 V, 0.59, and 1.94%, respectively.

2.6. IR spectra of 27-adsorbed zinc oxide

The IR spectra of **27** and **27**-adsorbed zinc oxide are shown in Fig. 9a and b. The carbonyl stretch band of **27** was clearly observed at 1720 cm^{-1} as shown in Fig. 9a. Meanwhile, this peak completely disappeared in **27**-adsorbed zinc oxide as shown in Fig. 9b. It is known that the intense carbonyl stretching band of esters is observed at around 1740 cm^{-1} and that those of asymmetrical and symmetrical stretch bands of

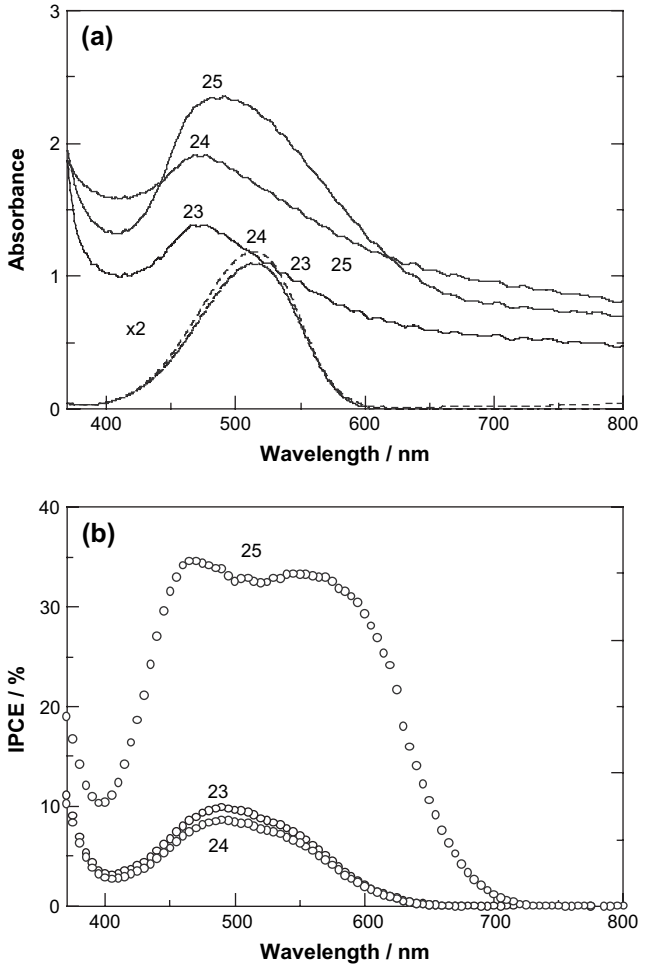

Fig. 5. (a) UV–vis absorption and (b) action spectra of **23**, **24**, and **25**. Solid and dotted lines represent the UV–vis absorption spectra on zinc oxide and in DMSO (1.0×10^{-5} mol dm^{-3}), respectively. The absorbance in DMSO is two-times large as measured.

carboxylates at around 1600 and 1400 cm^{-1}, respectively. These results suggest that the carboxyl group in **27** could adsorb on zinc oxide surface by bidentate carboxylate coordination and not the ester formation.

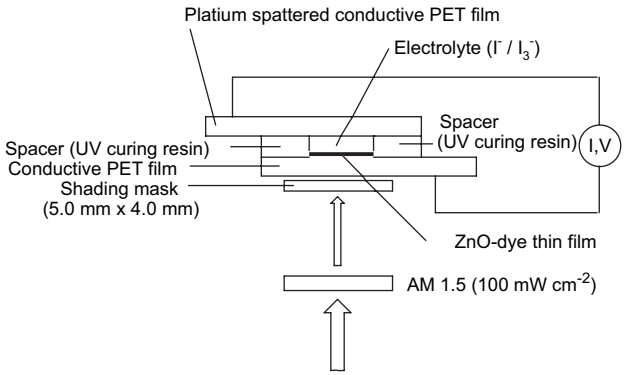

Fig. 6. Structure of flexible zinc oxide solar cell.

2.7. Thermal analysis of **27**

The TG–DTA curve of **27** is shown in Fig. 10. The endothermic peak of melting point was observed at 254 °C with a small endothermic peak at around 240 °C. The decrease in weight at around 240 °C was *ca*. 27%, which corresponds to evolution of a molar amount of hydroiodic acid.

3. Conclusion

Application of a series of styryl dyes for flexible zinc oxide solar cells prepared by the one-step cathode deposition template method was examined. 3-(2-Carboxyethyl)-2-[4-(dimethylamino)styryl]benzothiazolium iodide (**27**) was found to show the best performance as the sensitizer. After improvement of cell preparation, the IPCE at around 490 nm, J_{sc}, V_{oc}, ff, and η values were observed to be 54.5%, 6.22 mA cm^{-2}, 0.53 V, 0.59, and 1.94%, respectively. The dye can adsorb on zinc oxide surface by bidentate carboxylate coordination.

4. Experimental

4.1. Instruments

Melting points were measured with a Yanagimoto MP-52 micro-melting-point apparatus. NMR spectra were obtained by Varian Inova 500 spectrometers. EI and FABMS spectra were recorded on a JEOL MStation 700 spectrometer. UV–vis absorption and fluorescence spectra were taken on Hitachi U-3500 and F-4500 spectrophotometers, respectively. Cyclic voltammetry was carried out using an EG&G Princeton Applied Research Potentiostat/Galvanostat (Model 263A) driven by the M270 software package. IR spectra were measured with a Perkin–Elmer 2000 FTIR instrument.

4.2. Materials

2-Methylbenzothiazole (**1**), 2,3,3-trimethyl-3*H*-indolenine (**2**), 4-methylquinoline (**3**), 2,3,3-trimethyl-4,5-benzo-3*H*-indolenine (**4**), chloroacetic acid (**5**), bromoacetic acid (**6**), iodoacetic acid (**7**), 3-iodopropionic acid (**8**), and 4-(dimethylamino)benzaldehyde (**20**) were purchased from Tokyo Kasei Co., Ltd. Ethyl 4-bromobutyrate (**9**) and ethyl 5-bromovalerate (**10**) were purchased from Aldrich Co., Ltd. 4-(Dihexylamino) (**21**) and 4-(didodecylamino)benzaldehydes (**22**) were synthesized by a Vilsmeier–Haack reaction of the corresponding *N*,*N*-dialkylanilines.

4.3. Synthesis of N-(carboxyalkyl)-substituted heteroaromatic halides **11–15**, **16′**, **17′**, **18**, and **19**

To an acetonitrile solution (5 ml) of nitrogen-containing heteroaromatic compounds **1–4** (5 mmol) were added halo-substituted carboxylic acids **5–8** or esters **9** and **10** (6 mmol). The mixture was refluxed (**11**: 72 h; **12**, **15**, **18**, **19**: 24 h; **13**, **14**, **16′**, **17′**: 48 h). After cooling, the mixture

Table 2
Improvement of flexible zinc oxide solar cell performance

Run	Pre-electrolysis	Electrolysis temperature, °C	Immerse solvent	Washing of **27**-adsorbed ZnO	TBP[a]	J_{SC}[b], mA cm^{-2}	V_{OC}[b], V	ff[b]	η[b], %
1[c]	No	70	AN/*t*-BuOH	No	No	5.68	0.49	0.42	1.18
2	No	70	AN/*t*-BuOH	No	No	5.41	0.49	0.59	1.57
3	No	70	$CHCl_3$	No	No	5.91	0.52	0.53	1.63
4	Yes	70	$CHCl_3$	No	No	5.55	0.51	0.58	1.64
5	Yes	70	$CHCl_3$	No	Yes[d]	4.92	0.50	0.61	1.49
6	Yes	70	$CHCl_3$	Yes	No	6.21	0.51	0.54	1.71
7	Yes	50	$CHCl_3$	Yes	No	6.22	0.53	0.59	1.94

[a] 4-*tert*-Butylpyridine.
[b] Action spectrum under monochromatic light with 0.05×10^{16} photon cm^{-2} s^{-1} and I–V characteristics under white light with 100 mW cm^{-2}.
[c] Before improvement (run 5 in Table 1).
[d] TBP (0.05 mol dm^{-3}) was added to the electrolyte.

was poured into ether (300 ml). The resulting precipitate was filtered and washed with ether. In the case of **13**, the solvent was removed *in vacuo*. The crude product was used without further purification. In the cases of **16′** and **17′**, though a small amount of 2-methyl-3*H*-benzothiazolium bromide was present, the products were used without further purification. The physical and spectral data are shown below.

4.3.1. 3-(Carboxymethyl)-2-methylbenzothiazolium chloride (*11*)

Yield 63%; mp 209–211 °C; δ_H (500 MHz; DMSO-d_6; Me_4Si) 3.20 (3H, s), 5.79 (2H, s), 7.82 (1H, t, *J* 8.4), 7.90 (1H, t, *J* 8.4), 8.30 (1H, d, *J* 8.4), 8.49 (1H, d, *J* 8.4); *m/z* (EI) 207 (M^+ – HCl; 6%), 163 (100) and 148 (55).

4.3.2. 3-(Carboxymethyl)-2-methylbenzothiazolium bromide (*12*)

Yield 63%; mp 204–205 °C; δ_H (500 MHz; DMSO-d_6; Me_4Si) 3.21 (3H, s), 5.79 (2H, s), 7.81 (1H, t, *J* 8.1), 7.89 (1H, t, *J* 8.1), 8.30 (1H, d, *J* 8.1), 8.50 (1H, d, *J* 8.1); *m/z* (EI) 207 (M^+ – HBr; 52%), 163 (100), 162 (83) and 148 (87).

4.3.3. 1-(2-Carboxyethyl)-2,3,3-trimethyl-3H-indolium iodide (*14*)

Yield 40%; mp 185–186 °C; δ_H (500 MHz; DMSO-d_6; Me_4Si) 1.53 (6H, s), 2.86 (3H, s), 2.98 (2H, t, *J* 7.0), 4.65 (2H, t, *J* 7.0), 7.61–7.63 (2H, m), 7.83–7.85 (1H, m), 7.98–8.00 (1H, m), 12.72 (1H, br); *m/z* (EI) 231 (M^+ – HI; 73%), 216 (85), 174 (56), 144 (53) and 128 (100).

4.3.4. 3-(2-Carboxyethyl)-2-methylbenzothiazolium iodide (*15*)

Yield 85%; mp 246–247 °C; δ_H (500 MHz; DMSO-d_6; Me_4Si) 3.00 (2H, t, *J* 7.3), 3.27 (3H, s), 4.90 (2H, t, *J* 7.3), 7.86 (1H, t, *J* 8.3), 7.89 (1H, t, *J* 8.3), 8.37 (1H, d, *J* 8.3), 8.46 (1H, d, *J* 8.3), 12.75 (1H, br); *m/z* (EI) 211 (M^+ – HI; 2%), 149 (100), 128 (50) and 108 (31).

4.3.5. 3-(3-Ethoxycarbonylpropyl)-2-methylbenzothiazolium bromide (*16′*)

Yield 18%; δ_H (500 MHz; DMSO-d_6; Me_4Si) 1.16 (3H, t, *J* 7.5), 2.11 (2H, quint, *J* 7.5), 2.60 (2H, t, *J* 7.5), 3.21 (3H, s), 4.05 (2H, q, *J* 7.5), 4.72 (2H, t, *J* 7.5), 7.80–7.83 (1H, m), 7.90–7.93 (1H, m), 8.37 (1H, d, *J* 8.5), 8.45 (1H, d, *J* 8.5).

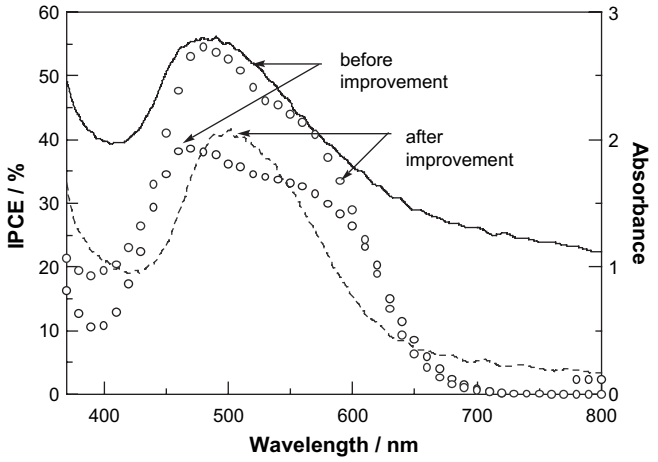

Fig. 7. UV–vis absorption and action spectra of **27** before and after improvement of cell performance.

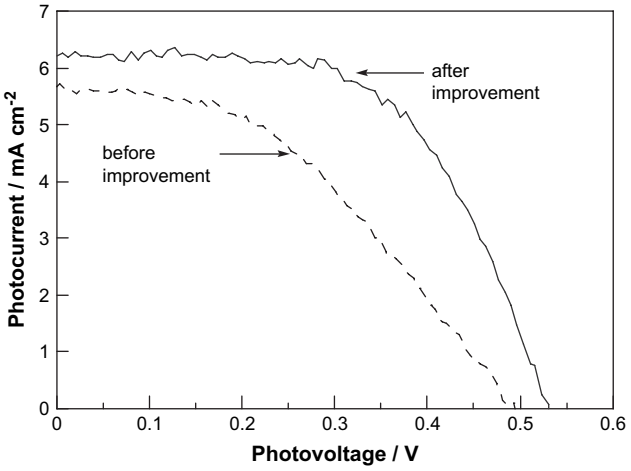

Fig. 8. Photocurrent density–photovoltage (I–V) curve of **27** before and after improvement of cell performance.

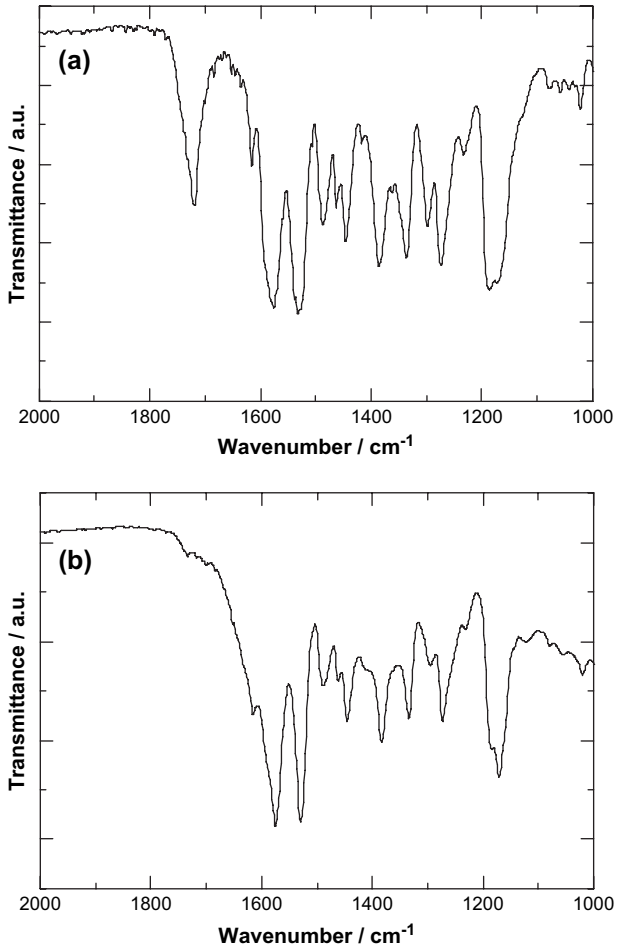

Fig. 9. IR spectra of **27** and **27**-adsorbed zinc oxide. Measure by KBr disk.

*4.3.6. 3-(4-Ethoxycarbonylbutyl)-2-methylbenzothiazolium bromide (**17′**)*

Yield 73%; δ_H (500 MHz; DMSO-d_6; Me_4Si) 1.16 (3H, t, *J* 7.5), 1.70 (2H, quint, *J* 7.5), 1.87 (2H, quint, *J* 7.5), 2.39 (2H, t, *J* 7.5), 3.20 (3H, s), 4.05 (2H, q, *J* 7.5), 4.74 (2H, t, *J* 7.5), 7.79–7.82 (1H, m), 7.88–7.91 (1H, m), 8.34 (1H, d, *J* 8.5), 8.44 (1H, d, *J* 8.5).

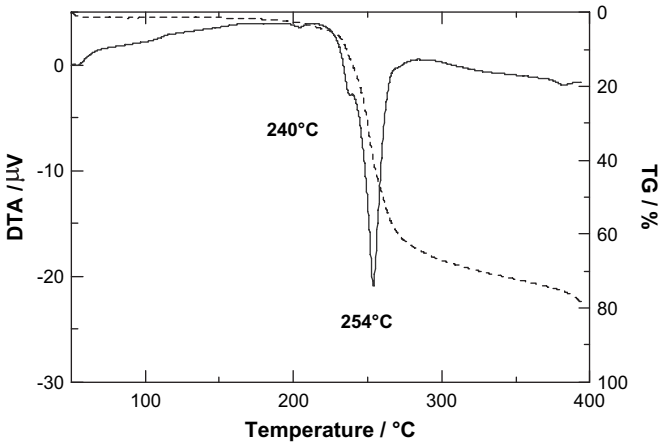

Fig. 10. TG–DTA curve of **27**.

*4.3.7. 1-(2-Carboxyethyl)-4-methylquinolinium iodide (**18**)*

Yield 76%; mp 182–183 °C; δ_H (500 MHz; DMSO-d_6; Me_4Si) 3.01 (3H, s), 3.06 (2H, t, *J* 6.8), 5.21 (2H, t, *J* 6.8), 8.06 (1H, t, *J* 8.1), 8.08 (1H, d, *J* 6.1), 8.26 (1H, t, *J* 8.1), 8.55 (1H, d, *J* 8.1), 8.61 (1H, d, *J* 8.1), 9.43 (1H, d, *J* 6.1); *m/z* (EI) 143 ($M^+ - IC_2H_4COOH$; 100%), 128 (50), 115 (32) and 72 (23).

*4.3.8. 1-(Carboxyethyl)-2,3,3-trimethyl-4,5-benzo-3H-indolium iodide (**19**)*

Yield 40%; mp 172–173 °C; δ_H (500 MHz; DMSO-d_6; Me_4Si) 1.76 (6H, s), 2.97 (3H, s), 3.05 (2H, t, *J* 7.0), 4.78 (2H, t, *J* 7.0), 7.75 (1H, t, *J* 7.7), 7.78 (1H, t, *J* 7.7), 8.18 (1H, d, *J* 9.2), 8.23 (1H, d, *J* 7.7), 9.29 (1H, d, *J* 9.2), 8.38 (1H, d, *J* 7.7); *m/z* (EI) 281 ($M^+ - HI$, 38%), 266 (100), 209 (29), 194 (44) and 128 (90).

*4.4. Synthesis of styryl dyes **16** and **17***

To a THF–dichloromethane mixed solvent (**16**: THF, 24 ml, CH_2Cl_2, 8 ml; **17**: THF, 38 ml, CH_2Cl_2, 13 ml) were added **16′** (806 mg, 1.83 mmol) or **17′** (1.433 g, 4.14 mmol) and 6 mol dm^{-3} of hydrochloric acid (**16**: 16 ml; **17**: 25 ml). The mixture was stirred at ambient temperature (**16**: 5 h; **17**: 10 min). After the reaction was completed, to the mixture were added water (**16**: 18 ml; **17**: 25 ml) and dichloromethane (**16**: 8 ml; **17**: 12.5 ml). The mixture was stirred again (**16**: 10 min; **17**: 5 h). The water layer was washed with dichloromethane (**16**: 8 ml × 3, **17**: 15 ml × 3) and ether (**16**: 8 ml, **17**: 15 ml). Water was evaporated *in vacuo* to give **16** and **17**. In the case of **16**, although it contained a small amount of unreacted 2-methyl-3*H*-benzothiazolium bromide, it was subsequently used without further purification. In the case of **17**, the crude product was washed with acetone again. The physical and spectral data are shown below.

*4.4.1. 3-(3-Carboxypropyl)-2-methylbenzothiazolium bromide (**16**)*

Yield 99%; δ_H (500 MHz; DMSO-d_6; Me_4Si) 1.98 (2H, quint, *J* 7.4), 2.43 (2H, t, *J* 7.4), 3.12 (3H, s), 4.63 (2H, t, *J* 7.4), 7.70–7.73 (1H, m), 7.80–7.84 (1H, m), 8.28 (1H, d, *J* 8.4), 8.36 (1H, d, *J* 8.4).

*4.4.2. 3-(3-Carboxybutyl)-2-methylbenzothiazolium bromide (**17**)*

Yield 46%; mp 217–219 °C; δ_H (500 MHz; DMSO-d_6; Me_4Si) 1.67 (2H, quint, *J* 7.6), 1.87 (2H, quint, *J* 7.6), 2.31 (2H, t, *J* 7.6), 3.21 (3H, s), 4.74 (2H, t, *J* 7.6), 7.79–7.82 (1H, m), 7.88–7.91 (1H, m), 8.35 (1H, d, *J* 8.5), 8.46 (1H, d, *J* 8.5).

*4.5. Synthesis of styryl dyes **23–29**, **30′**, **31′**, **32**, and **33***

To an ethanolic solution (5 ml) of the appropriate *N*-(carboxyalkyl)-substituted heteroaromatic halides **11–19** (1 mmol) were added piperidine (1 mmol) and the appropriate aromatic aldehydes **20–22** (1 mmol). The mixture was

refluxed for few hours. After the reaction was completed, the mixture was cooled to ambient temperature. To the solution was added ether (200 ml). The resulting precipitate was filtered, purified by silica gel column chromatography (**23**, **24**, **25**, **26**, **27**, **28**, **29**, **30′**, **32**, **33**: CH_2Cl_2:MeOH = 6:1; **31′**: CH_2Cl_2:MeOH = 3:1), filtered through BOND ELUTE-C18 to remove silica gel and recrystallized (**23**, **24**, **25**, **26**, **27**, **30′**, **31′**, **32**, **33**: methanol; **28**, **29**: ethanol). The physical and spectral data are shown below.

*4.5.1. 3-(Carboxymethyl)-2-[4-(dimethylamino)styryl]-benzothiazolium chloride (**23**)*

Yield 60%; mp 299–301 °C; δ_H (500 MHz; DMSO-d_6; Me_4Si) 3.09 (6H, s), 5.10 (2H, s), 6.82 (2H, d, *J* 9.2), 7.52 (1H, d, *J* 15.4), 7.62–7.66 (1H, m), 7.69–7.73 (1H, m), 7.86 (2H, d, *J* 9.2), 7.91 (1H, d, *J* 8.1), 7.99 (1H, d, *J* 15.4), 8.26 (1H, d, *J* 8.1); *m/z* (FAB) 339 ($M^+ - Cl$).

*4.5.2. 3-(Carboxymethyl)-2-[4-(dimethylamino)styryl]-benzothiazolium bromide (**24**)*

Yield 43%; mp 159–161 °C; δ_H (500 MHz; DMSO-d_6; Me_4Si) 3.09 (6H, s), 5.09 (2H, s), 6.82 (2H, d, *J* 9.2), 7.53 (1H, d, *J* 15.4), 7.62–7.66 (1H, m), 7.69–7.73 (1H, m), 7.86 (2H, d, *J* 9.2), 7.91 (1H, d, *J* 7.9), 8.00 (1H, d, *J* 15.4), 8.26 (1H, d, *J* 7.9); *m/z* (FAB) 339 ($M^+ - Br$).

*4.5.3. 3-(Carboxymethyl)-2-[4-(dimethylamino)styryl]-benzothiazolium iodide (**25**)*

Yield 15%; mp 214–216 °C; δ_H (500 MHz; DMSO-d_6; Me_4Si) 3.13 (6H, s), 5.72 (2H, s), 6.85 (2H, d, *J* 8.9), 7.64 (1H, d, *J* 15.0), 7.66–7.69 (1H, m), 7.74–7.77 (1H, m), 7.91 (2H, d, *J* 8.9), 8.01 (1H, d, *J* 8.2), 8.13 (1H, d, *J* 15.0), 8.31 (1H, d, *J* 8.2); *m/z* (FAB) 339 ($M^+ - I$).

*4.5.4. 1-(2-Carboxyethyl)-3,3-dimethyl-2-[4-(dimethylamino)styryl]-3H-indolium iodide (**26**)*

Yield 36%; mp 149–150 °C; δ_H (500 MHz; DMSO-d_6; Me_4Si) 1.72 (6H, s), 2.63 (2H, t, *J* 6.9), 3.14 (6H, s), 4.63 (2H, t, *J* 6.9), 6.86 (2H, d, *J* 8.9), 7.41 (1H, d, *J* 15.7), 7.44 (1H, t, *J* 7.5), 7.51 (1H, t, *J* 7.5), 7.67 (1H, d, *J* 7.5), 7.75 (1H, d, *J* 7.5), 8.04 (2H, d, *J* 8.9), 8.27 (1H, d, *J* 15.7); *m/z* (FAB) 363 ($M^+ - I$).

*4.5.5. 3-(2-Carboxyethyl)-2-[4-(dimethylamino)styryl]-benzothiazolium iodide (**27**)*

Yield 46%; mp 226–227 °C; δ_H (500 MHz; DMSO-d_6; Me_4Si) 2.75 (2H, t, *J* 7.0), 3.02 (6H, s), 4.89 (2H, t, *J* 7.0), 6.72 (2H, t, *J* 8.8), 7.63 (1H, t, *J* 7.9), 7.68 (1H, d, *J* 15.4), 7.73 (1H, t, *J* 7.9), 7.80 (2H, d, *J* 8.8), 7.96 (1H, d, *J* 15.4), 8.05 (1H, d, *J* 7.9), 8.21 (1H, d, *J* 7.9); *m/z* (FAB) 353 ($M^+ - I$).

*4.5.6. 3-(2-Carboxyethyl)-2-[4-(dihexylamino)styryl]-benzothiazolium iodide (**28**)*

Yield 35%; mp 204–205 °C; δ_H (500 MHz; DMSO-d_6; Me_4Si) 0.88 (6H, t, *J* 7.3), 1.31 (12H, br s), 1.56 (4H, quint, *J* 7.3), 2.87 (2H, t, *J* 7.2), 3.43 (4H, t, *J* 7.3), 4.92 (2H, t, *J* 7.2), 6.79 (2H, t, *J* 8.9), 7.64 (1H, d, *J* 15.2), 7.66 (1H, t, *J* 8.0), 7.75 (1H, d, *J* 8.0), 7.88 (2H, d, *J* 8.9), 8.04 (1H, d, *J* 15.2), 8.10 (1H, d, *J* 8.0), 8.27 (1H, d, *J* 8.0); *m/z* (FAB) 493 ($M^+ - I$).

*4.5.7. 3-(2-Carboxyethyl)-2-[4-(didodecylamino)styryl]-benzothiazolium iodide (**29**)*

Yield 42%; mp 144–145 °C; δ_H (500 MHz; DMSO-d_6; Me_4Si) 0.87 (6H, t, *J* 7.3), 1.30 (36H, br s), 1.55 (4H, br s), 2.88 (2H, t, *J* 6.3), 3.44 (4H, t, *J* 7.3), 4.81 (2H, t, *J* 6.3), 6.42 (2H, t, *J* 8.0), 7.40 (1H, t, *J* 7.4), 7.47 (1H, t, *J* 7.4), 7.50 (1H, d, *J* 15.5), 7.58 (1H, d, *J* 7.4), 7.64 (2H, d, *J* 8.0), 7.84 (1H, d, *J* 15.5), 8.11 (1H, d, *J* 7.4); *m/z* (FAB) 662 ($M^+ - I$).

*4.5.8. 3-(3-Carboxypropyl)-2-[4-(dimethylamino)styryl]-benzothiazolium bromide (**30′**)*

Yield 19%; mp 264–266 °C; δ_H (500 MHz; DMSO-d_6; Me_4Si) 2.04 (2H, quint, *J* 6.6), 2.53 (2H, t, *J* 6.6), 3.12 (6H, s), 4.75 (2H, t, *J* 6.6), 6.84 (2H, d, *J* 7.3), 7.66 (1H, d, *J* 15.1), 7.67–7.70 (1H, m), 7.78–7.81 (1H, m), 7.92 (2H, d, *J* 7.3), 8.10 (1H, d, *J* 15.1), 8.18 (1H, d, *J* 8.1), 8.31 (1H, d, *J* 8.1); *m/z* (FAB) 368 ($M^+ - Br$).

*4.5.9. 3-(4-Carboxybutyl)-2-[4-(dimethylamino)styryl]-benzothiazolium bromide (**31′**)*

Yield 61%; mp 236–238 °C; δ_H (500 MHz; DMSO-d_6; Me_4Si) 1.67 (2H, quint, *J* 7.3), 1.83 (2H, quint, *J* 7.3), 2.28 (2H, t, *J* 7.3), 3.11 (6H, s), 4.82 (2H, t, *J* 7.3), 6.84 (2H, d, *J* 9.0), 7.62 (1H, d, *J* 15.4), 7.66–7.69 (1H, m), 7.76–7.79 (1H, m), 7.93 (2H, d, *J* 9.0), 8.09 (1H, d, *J* 15.4), 8.14 (1H, d, *J* 8.2), 8.30 (1H, d, *J* 8.2); *m/z* (FAB) 381 ($M^+ - Br$).

*4.5.10. 1-(2-Carboxyethyl)-4-[4-(dimethylamino)styryl]-quinolinium iodide (**32**)*

Yield 32%; mp 147–148 °C; δ_H (500 MHz; DMSO-d_6; Me_4Si) 2.53 (2H, t, *J* 6.4), 3.06 (6H, s), 4.97 (2H, t, *J* 6.4), 6.82 (2H, d, *J* 7.4), 7.85 (2H, d, *J* 7.4), 7.93 (1H, t, *J* 8.2), 7.98 (1H, d, *J* 15.6), 8.11 (1H, d, *J* 15.6), 8.16 (1H, t, *J* 8.2), 8.26 (1H, d, *J* 5.8), 8.40 (1H, d, *J* 8.2), 8.98 (1H, d, *J* 8.2), 9.17 (1H, d, *J* 5.8); *m/z* (FAB) 347 ($M^+ - I$).

*4.5.11. 1-(2-Carboxyethyl)-3,3-dimethyl-2-[4-(dimethylamino)styryl]-4,5-benzo-3H-indolium iodide (**33**)*

Yield 48%; mp 233–234 °C; δ_H (500 MHz; DMSO-d_6; Me_4Si) 1.97 (6H, s), 2.76 (2H, t, *J* 6.6), 3.15 (6H, s), 4.78 (2H, t, *J* 6.6), 6.87 (2H, d, *J* 8.8), 7.43 (1H, d, *J* 15.9), 7.64 (1H, t, *J* 7.8), 7.75 (1H, t, *J* 7.8), 7.94 (1H, d, *J* 8.8), 8.07 (2H, d, *J* 8.8), 8.14 (1H, d, *J* 7.8), 8.18 (1H, d, *J* 8.8), 8.33 (1H, d, *J* 7.8), 8.39 (1H, d, *J* 15.9); *m/z* (FAB) 413 ($M^+ - I$).

*4.6. Synthesis of **30** and **31***

To a methanol–chloroform mixed solvent (**30**: MeOH, 4 ml, $CHCl_3$, 1 ml; **31**: MeOH, 20 ml, $CHCl_3$, 5 ml) was added a methanol–chloroform mixed solution (methanol: 4 ml, chloroform: 1 ml) of **30′** (160 mg, 0.36 mmol) or **31′** (231 mg,

0.50 mmol). The mixture was heated to dissolve the substrate. The solution was filtered. To the filtrate was added aqueous potassium iodide (**30**: 1 mol dm^{-3}, 3.5 ml; **31**: 2.5 mol dm^{-3}, 2 ml). The mixture was refluxed for 1.5 h and filtered. The filtrate was concentrated *in vacuo* until 3 ml. Then, the product was purified by silica gel column chromatography (CH_2Cl_2:MeOH = 6:1). The eluent was filtered through BOND ELUT-C18 to remove silica gel and recrystallized from methanol.

*4.6.1. 3-(3-Carboxypropyl)-2-[4-(dimethylamino)styryl]-benzothiazolium iodide (**30**)*

Yield 97%; mp 252–254 °C; δ_H (500 MHz; DMSO-d_6; Me_4Si) 2.00 (2H, quint, *J* 7.2), 2.42 (2H, t, *J* 7.2), 3.07 (6H, s), 4.72 (2H, t, *J* 7.2), 6.79 (2H, d, *J* 8.7), 7.67 (1H, d, *J* 15.3), 7.75–7.79 (2H, m), 7.91 (2H, d, *J* 8.7), 8.05 (1H, d, *J* 15.3), 8.21 (1H, d, *J* 8.1), 8.29 (1H, d, *J* 8.1); *m/z* (FAB) 368 ($M^+ - I$).

*4.6.2. 3-(4-Carboxybutyl)-2-[4-(dimethylamino)styryl]-benzothiazolium iodide (**31**)*

Yield 63%; mp 257–259 °C; δ_H (500 MHz; DMSO-d_6; Me_4Si) 1.67 (2H, quint, *J* 7.3), 1.84 (2H, quint, *J* 7.3), 2.30 (2H, t, *J* 7.3), 3.12 (6H, s), 4.82 (2H, t, *J* 7.3), 6.86 (2H, d, *J* 8.9), 7.61 (1H, d, *J* 15.1), 7.67–7.70 (1H, m), 7.76–7.79 (1H, m), 7.93 (2H, d, *J* 8.9), 8.10 (1H, d, *J* 15.1), 8.14 (1H, d, *J* 8.3), 8.31 (1H, d, *J* 8.3); *m/z* (FAB) 381 ($M^+ - I$).

4.7. Electrochemical properties of styryl dyes

Since dyes **23–33** were less soluble in acetonitrile, cyclic voltamogram was measured in DMSO. The oxidation potential (E_{ox}) was measured *vs* Ag quasi-electrode. Dye **34** was less soluble in DMSO to perform electrochemical measurements. The E_{ox} of **27** was observed at 0.74 V *vs* Ag in DMSO. The E_{ox} of ferrocene which is usually used as a standard compound in the electrochemical measurements was observed at 0.70 V *vs* Ag in DMSO. The E_{ox} of ferrocene was observed at 0.48 V *vs* SCE in acetonitrile. Therefore, the E_{ox} of dyes *vs* SCE in acetonitrile is obtained according to an Eq. (1).

$$E_{ox}(\text{V vs SCE in acetonitrile}) = E_{ox}(\text{V vs Ag in DMSO}) - 0.22(\text{V}) \quad (1)$$

where E_{ox} (V *vs* SCE in acetonitrile) and E_{ox} (V *vs* Ag in DMSO) represent the E_{ox} *vs* SCE in acetonitrile and E_{ox} *vs* Ag in DMSO, respectively. Thus, the E_{ox} of **27** was calculated to be 0.52 V *vs* SCE in acetonitrile.

The reduction potential (E_{red}) was obtained on the basis of the E_{ox} and onset wavelength (λ_{onset}) of dye on zinc oxide. For example, the λ_{onset} of **27** was observed at around 706 nm as shown in Fig. 1, corresponding to 1.76 V. Therefore, the E_{red} was calculated to be −1.24 V *vs* SCE in acetonitrile.

4.8. Electrochemical measurements

A DMSO solution (5 ml) of dye (5×10^{-4} mol dm^{-3}) containing tetrabutylammonium perchlorate (0.1 mol dm^{-3}) was used as an electrolyte. The oxidation potential (E_{ox}) was measured by using three small-size electrodes. The electrochemical measurement was performed at the scan rate of 100 mV s^{-1}.

Acknowledgement

This work was financially supported in part by Grants-in-Aid for Science Research (No. 17550172) from Japan Society for the Promotion of Science (JSPS).

References

[1] Arakawa H. New technology in dyes-sensitized solar cells. Tokyo: CMC; 2001. and literatures cited therein.
[2] Hara K, Kurashige M, Dan Y, Kasada C, Shinpo A, Suga S, et al. Design of new coumarin dyes having thiophene moieties for highly efficient organic-dye-sensitized solar cells. New J Chem 2003;27:783–5.
[3] Sayama K, Tsukagoshi S, Hara K, Ohga Y, Shinpo A, Abe Y, et al. Photoelectrochemical properties of J aggregates of benzothiazole merocyanine dyes on a nanostructured TiO_2 film. J Phys Chem B 2002;106:1363–71.
[4] Hara K, Kurashige M, Ito S, Shinpo A, Suga S, Sayama K, et al. Novel polyene dyes for highly efficient dye-sensitized solar cells. Chem Commun 2003;252–3.
[5] Horiuchi T, Miura H, Uchida S. Highly-efficient metal-free organic dyes for dye-sensitized solar cells. Chem Commun 2003;3036–7.
[6] Wang Z-S, Li F-U, Huang C-H. Highly efficient sensitization of nanocrystalline TiO_2 films with styryl benzothiazolium propylsulfonate. Chem Commun 2000;2063–4;
Wang Z-S, Li F-U, Huang C-H. Photocurrent enhancement of hemicyanine dyes containing RSO_3^- group through treating TiO_2 films with hydrochloric acid. J Phys Chem B 2001;105:9210–7.
[7] Sayama K, Arakawa H, Hara K, Suga S, Shinho A, Oga Y. Semiconductor electrode using styryl dye photosensitizer, photoelectric conversion device and solar cell. JP. Pat. 234133, 2003. Chem Abstr 2003;139:182865.
[8] Lindström H, Holmberg A, Magnusson E, Malmqvist L, Hagfeldt A. A new method to make dye-sensitized nanocrystalline solar cells at room temperature. J Photochem Photobiol A Chem 2001;145:107–12.
[9] Kado T, Yamaguchi M, Yamada Y, Hayase S. Low temperature preparation of nano-porous TiO_2 layers for plastic dye sensitized solar cells. Chem Lett 2003;32:1056–7.
[10] Uchida S, Tomiha M, Takizawa H, Kawaraya M. Flexible dye-sensitized solar cells by 28 GHz microwave irradiation. J Photochem Photobiol A Chem 2004;164:93–6.
[11] Zhang D, Yoshida T, Furuta K, Minoura H. Hydrothermal preparation of porous nano-crystalline TiO_2 electrodes for flexible solar cells. J Photochem Photobiol A Chem 2004;164:159–66.
[12] Miyasaka T. Low-temperature fabrication of dye-sensitized plastic electrodes by electrophoretic preparation of mesoporous TiO_2 layers. J Electrochem Soc 2005;151:A1767–73.
[13] Halme J, Saarinen J, Lund P. Spray deposition and compression of TiO_2 nanoparticle films for dye-sensitized solar cells on plastic substrates. Sol Energy Mater Sol Cells 2006;90:887–99.
[14] Kakiuchi K, Hosono E, Fujiwara S. Enhanced photoelectrochemical performance of ZnO electrodes sensitized with N-719. J Photochem Photobiol A Chem 2006;179:81–6.
[15] Yoshida T, Iwaya M, Ando H, Oekermann T, Nonomura K, Schelettwein WD, et al. Improved photoelectrochemical performance

of electrodeposited ZnO/Eosin Y hybrid thin films by dye re-adsorption. Chem Commun 2004;400–1.

[16] Hara K, Wang A-S, Sato T, Furube A, Katoh R, Sugihara H, et al. Oligothiophene-containing coumarin dyes for efficient dye-sensitized solar cells. J Phys Chem 2005;109:15476–82.

[17] Kitamura T, Ikeda M, Shigaki K, Inoue T, Anderson NA, Ai X, et al. Phenyl-conjugated oligoene sensitizers for TiO_2 solar cells. Chem Mater 2004;16:1806–12.

[18] Herz AH. Dye–dye interactions of cyanines in solution and at AgBr surface. Photogr Sci Eng 1974;18:323–35.